Volume XXI 2018
ISSUE no.1
MBNA Publishing House Constanta 2018

Scientific Bulletin of Naval Academy

SBNA PAPER • OPEN ACCESS

Consideration on amorphic metals

To cite this article: A. Chioibas, Scientific Bulletin of Naval Academy, Vol. XXI 2018, pg. 468-482.

ISSN: 2392-8956; ISSN-L: 1454-864X

doi: 10.21279/1454-864X-18-I1-071

CONSIDERATION ON AMORPHIC METALS

A. Chioibas

Lecturer eng., Ph D, Naval Academy "Mircea cel Bătrân", Constanţa, România
e-mail: chioibasaura@yahoo.com

Abstract. Generally, following the rapid cooling of a molten metal, it reaches amorphous state, which is characterized by a disordered particle distribution. The structure of liquids is described by quasicrystalline theory. It considers that in a chemically and topographically restricted area, an amorphous metal is characterized by an ordered arrangement of the molten metal particles and is called a cluster (local order domain). Those alloys that have the high capacity to become amorphous, according to the positional criteria of the components in the periodic table of the elements, are analyzed.

1. Introduction

These materials are of particular interest to their magnetic properties. These properties are imprinted by the structure, reason why in this paper are analyzed combinations of different chemical elements, specific to the amorphous metals. Also, the properties are determined by thermal treatments applied to them.

2. Considerations regarding the liquid state of metallic materials

The amorphous state of metallic materials is obtained in most cases following the rapid cooling of a melt and corresponds to a disordered particle distribution.

2.1. Liquid state theories

Liquid state is a state of stable aggregation of matter. For the liquid state, it was not possible to construct an "ideal model" such as gases and solids, because the energy due to the interatomic forces of the particles and the thermal energy have a very close weight.

The liquid state can be achieved by cooling some gases or by heating solids above the melting temperature. In the case of solid state, the particles have an oscillatory motion around the nodes of the crystalline network, so a continuous vibration. In the case of gases, the continuous and disorderly translational movement of the particles is predominant. In fluid there is a composite motion of the particles between disordered translation and vibration, explained by several theories presented below.

2.1.1. Theory of the kinetic model. This theory is based on the Van der Waals gas-specific model [2, 4]. Thus, molecules are considered as material points in continuous disordered motion. In their rectilinear movements, the molecules collide with each other, changing their direction and speed after each collision. The clashes of the molecules being perfectly elastic, their kinetic energy stays constant (at constant temperature).

According to the kinetic theory, for the ideal gas the equation is valid:

$$pV = \nu RT. \tag{1}$$

The real gases have a different behavior than the ideal ones, for which the Van de Waals state equation is valid:

$$\left[p + \left(\frac{a}{V^2}\right)\right](V - b) = \nu RT, \tag{2}$$

At high pressures, the own volume of gas molecules is no longer negligible, as evidenced by constants a and b.

At high pressures the volume of gas is lower than the volume calculated for an ideal gas, between molecules there are forces of attraction. The gas is compressed as if under a higher pressure than the Boyle-Mariotte law.

The state of the gas depends on its temperature and pressure. The behavior of the real gas over the ideal gas is evidenced by the isothermal curves $p = f(V)$. In Figure 1 [4] shows the change of the real gas state according to pressure and temperature. At different temperatures, the $p{\cdot}V$ curves will have different shapes; at temperature rise over critical ($T_n > T_I > T_{cr}$) the $p{\cdot}V$ curve approaches the shape of a hyperbole, according to Boyle-Mariotte's law. In zone I there is only gas, in zone II there is only liquid and in III there is gas and liquid. The isotherm at critical temperature has a inflection point I. At $T_2 < T_{cr}$ isothermal shows almost vertical DC (volume does not change with increasing pressure) and a liquid state appears. The CB branch (horizontal which shows that the pressure remains constant) corresponds to the coexistence of the gas with the liquid and the BA branch shows that the volume increases and the pressure decreases, approximate according to Boyle-Mariotte's law. At point B the liquid is completely transformed into gas.

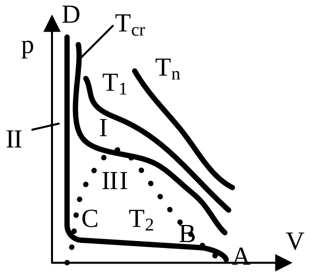

Fig.1. Isothermal pV curves for real gas

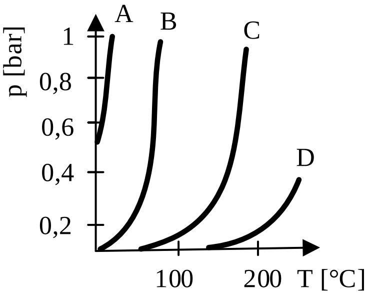

Fig.2. Real gas pressure variation with temperature

Van der Waals theory admits the existence of weak forces of attraction between compressed gas molecules, unforeseen forces in kinetic theory.

For various chemical elements A ... D (Figure 2 [4]) it is observed that the variation of gas pressure with temperature is made after a hyperbola.

Van de Waals's theory of real gas partially explains the liquid state of the material. According to this theory, the liquid appears as a compressed gas, in which molecules move randomly on an average free path. The molecules in the liquid state respect - in micro-volume, at small distances - an arrangement according to certain laws, compared to the random situation in the gases. The compressibility of the liquids is closer to that of the solids than the gaseous state. The mass heat of the liquid state are deviated from the gaseous state and very close to those of the solid state, and at melting temperature have almost identical values. In the liquid and solid state there is almost the same number of coordinates. In the solid state, the particles have maximum kinetic energy in the equilibrium positions and maximum potential energy in the positions that deviate from the balance of the network. In the liquid, the sum of the kinetic energy of the particles exceeds the potential energy of the solid, and the crystalline network crumbles.

The above described gaseous and liquid states lead to the conclusion that the kinetic model theory can't be applied to liquids, which is why the quasi-crystalline model (cluster model) is chosen.

2.1.2. Theory of the quasi-crystalline model. The suggestive description of the fluid structure is made using the clustered network model, also called the quasi-crystalline model. The cluster name also has synonyms such as "local order domain", "structural quant".

In a poly-component liquid, the cluster represents a relatively stable set of atoms with stronger internal links than the outside ones (between neighboring clusters). The cluster has no well-defined limits and is unstable. The existence of the cluster is temporary; they are destroyed in one place and they are immediately restored to another, they can move from one position of balance to another by leaps or translations. Cluster decomposition leads to a change in the atomic coordination number, it is not related to certain status parameters and has a continuous character. The decomposition of the clusters and their displacement explain the fluidity of the liquids.

According to the structural model of the Fränkel type, the liquid consists of clusters separated from each other by numerous spaces where the density is lower than in the rest of the structure, similar to voids. Increasing the temperature makes these voids grow in volume and mobility, so they migrate inside the melt.

To explain the liquid state, Fränkel introduces two time parameters: t_0 - the "sedentary" time of the cluster, that is, the time in which it is in balance; t - the "active life" time in which the cluster moves. Corresponding to the molecular vibration frequency t = 10 -12s, while t_0 = 10- 7s (with several orders of magnitude higher than t). Time t_0 determines the equilibrium properties, the quasi-equilibrium state of the liquid, and time t explains the fluidity of the liquid. The macroscopic viewing time of the liquid is t_1, which is much higher than the value t_0.During this time t_1 takes place a large number of molecule displacements and the observer perceives the liquid as a fluid. If liquid perception would be done during t_0, then the liquid would appear as a solid. This fact was confirmed by the research of adiabatic compression fluid, made at ultrasound speed. Analyzing the variance of adiabatic compression χ_s according to the ultrasonic frequency used (Figure 3 [4]), it is observed that χ_s remains constant over a wide range of frequencies. When the duration of the ultrasonic impulse is very low, of the order t_0 = 10- 7s, the liquid behaves like a solid. The state of order and / or clutter of atoms in a body is evidenced by X-radiation χ_s.

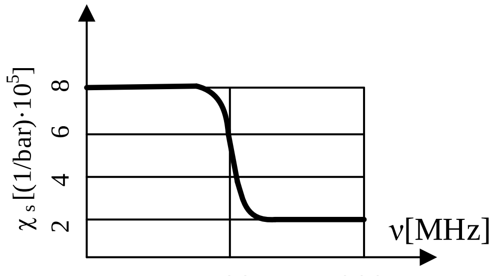

Fig. 3. Variation of adiabatic fluid compressibility according to ultrasonic frequency

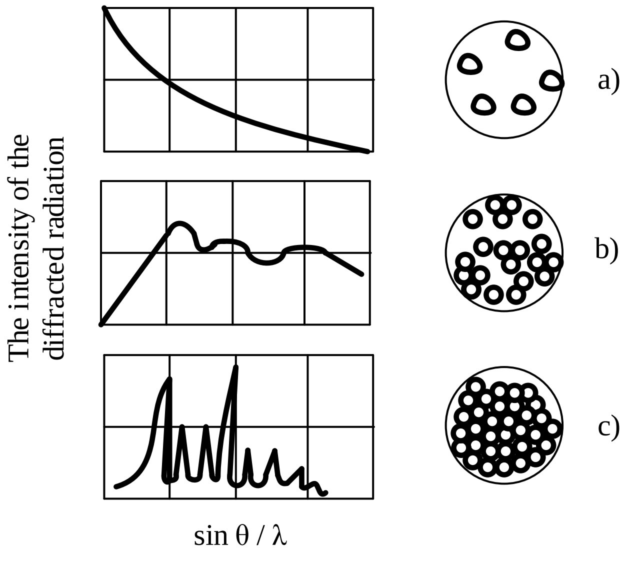

Fig. 4. Analyzed X-ray aggregation states: a) gaseous state - total disordered particle arrangement; b) the liquid state - a small order arrangement of the atoms (partial disorder); c) solid state - arrangement of atoms with long-distance order

By comparing the diffraction images of the three states of aggregation (Figure 4 [4]), in the case of the liquid, the order is shown at a small distance, so quasi-crystalline theory is confirmed with some certainty.

The quasi-crystalline models of liquids are also confirmed by the fact that:

1) The compressibility of liquids is of the same magnitude as the solids. The compressibility of liquids (χl) is approximately four times higher than solids χ_s and 10^6 times less than gas.
2) The caloric capacities of the liquids are of the same order of magnitude as the solids, near the melting temperature.
3) 3) The vibrations of the molecules of a liquid in the temporary equilibrium position are about 10^{12} ... 10^{13} vibrations/s, i.e. very close to those of the solid state. This suggests that the density of intermolecular forces and the structure of the two states are very close.

On heating, due to the thermal agitation that is higher for liquids than for solids, the structural arrangement changes slightly after melting and also the cohesion forces between the molecules weaken to some extent. All of these experimental data confirm that the liquid structure is closer to solids than to the gases.

In addition to this structural model, a complete description of the fluid structure involves the realization of mathematical models [3].

3. The amorphous state of metallic materials

Below is analyzed the vitreous transition phenomenon for metallic materials, some theories on amorphous state of metallic materials, as well as the capacityof alloys to become amorphous.

3.1.Considerations on solidification processes

Solidification of the melts requires mass and thermal transport processes. Mass transport is achieved by diffusion and convection. Melt agitation causes convection currents due to hydrodynamic movements produced by the fluid jet, density differences between different melt areas, gas bubble exhausts, and the like. Thermal transport is influenced by the release of latent heat of solidification and the thermal gradient of the melt.

Solidification of the melts requires mass and thermal transport processes. Mass transport is achieved by diffusion and convection. Melt agitation causes convection currents due to hydrodynamic movements produced by the fluid jet, density differences between different melt areas, gas bubble exhausts, and the like. Thermal transport is influenced by the release of latent heat of solidification and the thermal gradient of the melt. To achieve melting or solidification it is necessary to vary the free energy of the system, which is obtained by changing the temperature. The driving force of transformation is the difference of the free energies ΔF of the two phases, liquid and solid. This energy difference of the system will be equal to the sum of system phase energies. Phase energies are influenced by germ size and temperature.

Dependence of ΔF size on the size of germs is expressed by the relationship:

$$\Delta F = -\left(\frac{4}{3}\right)\pi\Delta F_m r^3 + 4\pi\Delta F_s r\,. \tag{3}$$

For a certain degree of subtraction ΔT, the variation of ΔF according to the radius "r" is shown in Figure 5 [8]. It can be noticed that the energy difference of the system ΔF has a maximum corresponding to the critical size r_{cr}. The critical range of the germ is determined by relation:

$$r_{cr} = 2\frac{\Delta F_s}{\Delta F_m}\,, \tag{4}$$

where: ΔFs - the energy difference at the system phase limit; ΔF_m - the interphasicenergy difference of the system. The germs with $r < r_{cr}$ resolves in the melt, because by increasing them, an increase in the free energy of the system (see Figure 5).

The variation of the critical size according to the degree of subcooling ΔT is represented in Figure 6 [8] and is given by the relationship:

$$r_{cr} = \frac{2F_S \cdot M}{L_S \cdot \rho} \cdot \frac{T_e}{\Delta T} \ , \quad (5)$$

where: M / ρ - molar volume; L_s- latent solidification heat; T_e - the phase equilibrium temperature.

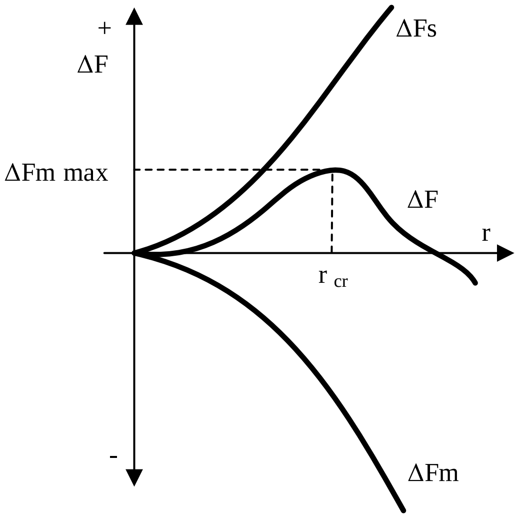

Fig. 5. The influence of the degree of subcooling on the free energy and the size of the germ; ΔFs – the energy difference at the system phase limit; ΔFm - the interphase energy difference of the system

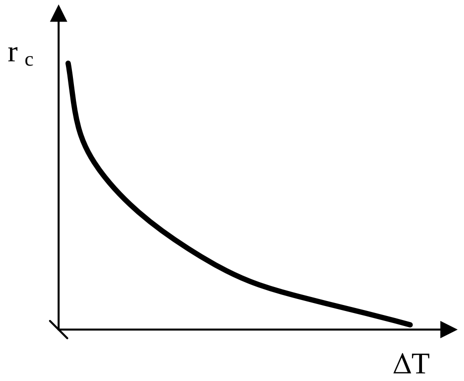

Fig. 6. Variation of the critical size of the germ depending on the degree of subtraction

It is noticed that for $\Delta T = 0$ it results $r_{cr} \rightarrow \infty$ and as such there is no solidification. For $\Delta T \rightarrow \infty$ (very high) results $r_{cr} \rightarrow 0$ (and although the state of aggregation changes, crystals are not formed, but the state of the melt is fixed, a state that tends to amorphous.

Therefore, the energetic conditions of the solidification can lead to the formation of crystals from the melt or to obtain a solid state in which the atoms have melt positions and a vitreous or amorphous state occurs.

3.2. The vitreous transition phenomenon for metallic materials

Increasing the degree of subcooling or cooling speed applied to the melt leads to the passage from the liquid phase to the solid phase, but the solid does not have the atoms arranged according to the model of a crystalline network of metallic materials, but presents an arrangement corresponding to the melt and a vitreous transition occurs. The vitreous state being a subcooling melt will present a cluster structure, thus a short distance order.

The transition from the liquid state to the vitreous state is not accompanied by a sudden variation in volume or a thermal effect as in the case of crystallisation (Figure 7 [6]).

In Figure 8 [6] was the temperature variation in function of time for various degrees of subcooling/supercooling applied to the melt. It can be noticed that a small degree of subcooling, marked ΔT_1, records a plateau region corresponding to the solidification temperature (Figure 8, a). Increasing the degree of subcooling (ΔT_2) leads to the attenuation of plateau region (Figure 8, b) or even its disappearance (ΔT_3). For high degree of subcooling or cooling speed, due to the non-compensation of heat loss, a variable slope appears instead of the plateau region, proof that no crystals ($T_c \ldots T_x$) have formed.

The critical cooling speed that does not allow the creation of crystals at solidification is calculated with the relationship [2]:

$$v_{cr} = Z\left(\frac{T_f}{t}\right), \qquad (5)$$

where: Z - constant; $t = \frac{\eta V}{K N_A T_f}$, relaxation time of kinetic units; η - viscosity index; V - molar volume; N_A - Avogadro's number; K - constant; T_f - melting temperature.

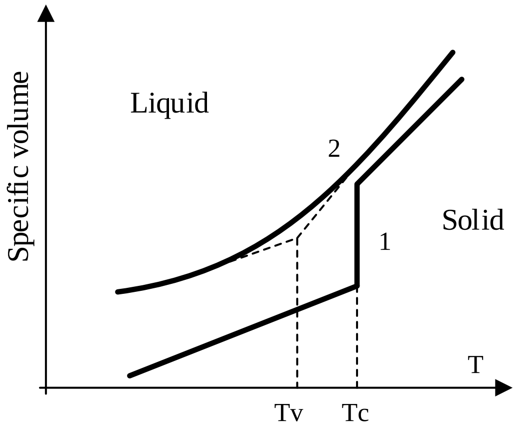

Fig. 7. Variation of the specific volume depending on the temperature, when passing from the liquid state to the crystalline or vitreous state; 1 - crystalline state; 2 - amorphous state

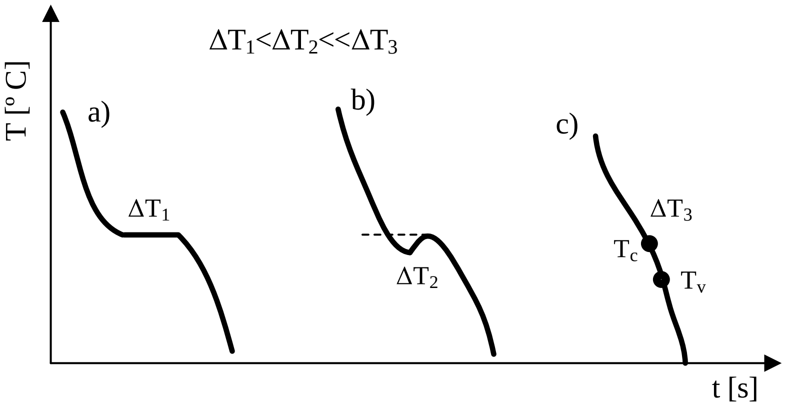

Fig. 8. Curbe de racire: a) grad de subracire mic; b) grad de subracire mare; c) grad de subracire foarte mare

Therefore, in order not to form crystals, the melt will have to be cooled at a speed higher than v_{cr} calculated with relation (5).

The vitreous solidification is realizing by applying melt cooling speed, which velocities will have to be large enough to prevent formation of crystallization germs and diffuse mass transport. The amorphous transformation is realizing in a temperature range ($T_c \dots T_v$), which includes the vitreous transition temperature (T_g).Amorphous solidification occurs when rapid melt cooling occurred under the temperature T_g. The value of the cooling speed between T_f and T_g depends on the nature of the melt and the cooling technique used.Experimental data show that cooling with $10^5 \dots 10^{10}$°C/s ensures the energetic conditions of melting "freezing" and amorphous metals obtaining.In conclusion, obtaining the vitreous transition is dependent on the cooling speed (degree of undercooling) used by the metal melt structure (which actually determines the amorphizing capacity of the metallic materials).

3.3. Theories on amorphous state of metallic materials

As has been shown, an X-ray analysis highlights a disordered arrangement of atoms in amorphous metals, or rather, an order at a small distance of atoms on a restricted range of 15 ... 20Å. This "order" is determined by the conditions of geometric nature and the chemical bonds of the particles.

The amorphous state of materials is appreciated on the basis of different structural and mathematical models.

3.3.1 The quasi-crystalline model. According to this model [4; 7], the amorphous metal is characterized by an orderly arrangement of the particles in a narrow range, from a chemical and topological point of view. This arrangement is genetically derived from the melt used to make amorphous metal [1]. It is hypothesized that the melt clusters form micro-volumes that show a small distance order. This local order is identical to a crystalline intermetallic compound - also called the second phase of the material.

Research [9; 10] conducted on Fe-B, Pb-Fe-P, Nb-Si-Ge alloys shows that phase II plays an important role in the amorphous metal structure.

Rapid cooling of the melt makes it possible in a solid state to form a cluster and hollow structure which leads to the production of metastable intermetallic compounds.

3.3.1.1. The type RPMU (Random Packing at Molecular Units). Taking into account the quasi crystalline model of amorphous metals, different types of particle arrangement have been created. This type is based on the idea that the metalloid atoms are surrounded by metal atoms disposed in a triangular prism geometric configuration (Figure 9)

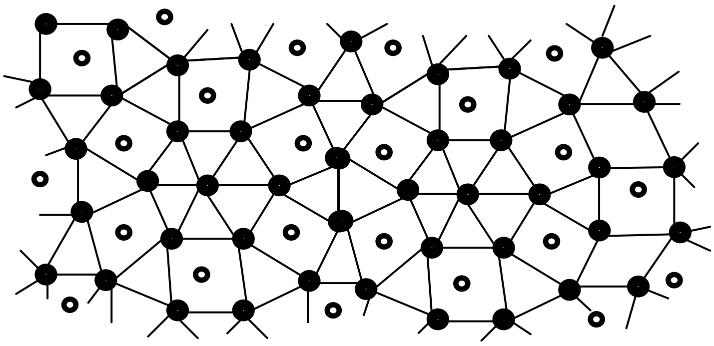

Fig. 9. Type of structure RPMU

At the RPMU type, the "molecule" consists in arranging the metalloid atoms in the center of a square and the metal atoms are arranged at the vertices of triangles associated with the square (Figure 9 [8]). It is assumed that the interatomic bonds are identical to the crystalline state and the metalloid atom is surrounded by the 8 metal atoms (Figure 9 [8]). It can be noticed that the order of atomization is kept at small distances (around the metalloid atoms). The elementary cell of the RPMU type, which is a triangular prism, is found in the structure of a large number of crystalline chemical compounds. This leads to the appearance of insignificant differences between the structures of various amorphous metals, which is a "minus" of the RPMU type.

3.3.1.2. The type DRP (Dense Random Packing) is the type of accidental dense packing of atoms. This type implies the existence of the local order imposed by geometric restrictions and the exclusion of the metalloid-metalloid strong contacts.

A variant of this type assumes that the transition metal atoms forms a strong sphere structure, and the metalloid atoms occupy the remaining large voids. Another variant (Bennett) admits that an existing cluster joins three atoms located at the minimum distance from the cluster's momentary center of gravity and forms spherical shapes that give a certain density of packing. Thus, a final spherical cluster is formed which presents a packing mean. Density decreases as it moves away from the center of the cluster and tends to infinity.

In another variant, it is believed that in the formation of the final cluster, the atoms to be clustered occupy only such positions in which the three spheres are at a distance from each other smaller than the size $K \cdot d_0$, where d_0 - the diameter of the sphere, $K = 1.06 \div 2$; if $K = 1$, the position of atoms occupies knots in ideal tetrahedrons; if $K = 2$, then the Bennett type is obtained.

Another proposes a dense packing model of rigid spheres and spokes, in which the spoke length corresponds to the atom distribution function in liquefied argon. Within the limits of a certain sphere, statistically N points were distributed and each point is considered the center of a small sphere with radius r_1. If two spheres are overlapping, then they move along the line that joins the centers to eliminating all overlapping.

The type of DRP in Figure 10 [8] comprises the metalloid atoms represented by hollow circles, the metal atoms in full circles, and the broken lines defining the nearest neighbor polyhedron.

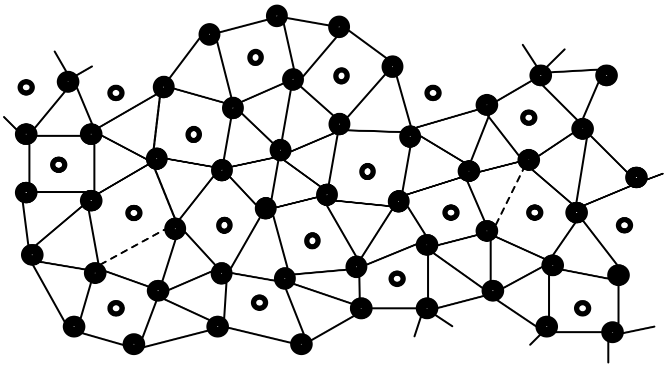

Fig. 10. Type of structure DRP

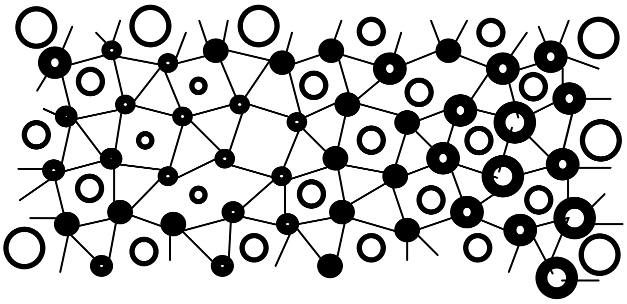

Fig. 11. Type of structure QC

3.3.1.3 The type of relaxation QC (Figure 11 [8]) assumes that the atom is no longer represented by a rigid sphere, and it allows the description of the interaction between atoms through their potentials that depend on distance. Each atom is moved to a position which ensures minimal energy, positions that depend on the other atoms.

In Figure 11 [8] atom 1 is the origin of the cluster, and the size of the circles is the significant probability of arranging other atoms.

Each of the above types is based on the quasi-crystalline model specific to the melt structure and admits that the amorphous state is generated by the liquid state of the metallic material.

3.4.The capacity of alloys to become amorphous

In the theory of liquid state (within which the glass transition was also explained) it is considered that any melt of metallic materials can be transformed into an "amorphous metal" if the cooling has been conducted at a velocity sufficiently high that the diffusion speeds are small, respectively the viscosity so high that formation of the crystalline germs and their growth does not take place. Interesting alloys with high capacity to become amorphous at maximum cooling speeds, achievable in industrial practice, are close to 10^{10} °C/s. This constraint applied to the melt leads to a reduction in the notion of amorphous metal to the alloys at which the cooling speeds of 10^6 ... 10^{10}°C/sassure the transition to amorphous state. Further reference will be made in particular to amorphous metals obtained by ultra-rapid cooling of the melt, of broad practical interest, from which they are obtained in the form of yarns, fibers, strips and good productivity.

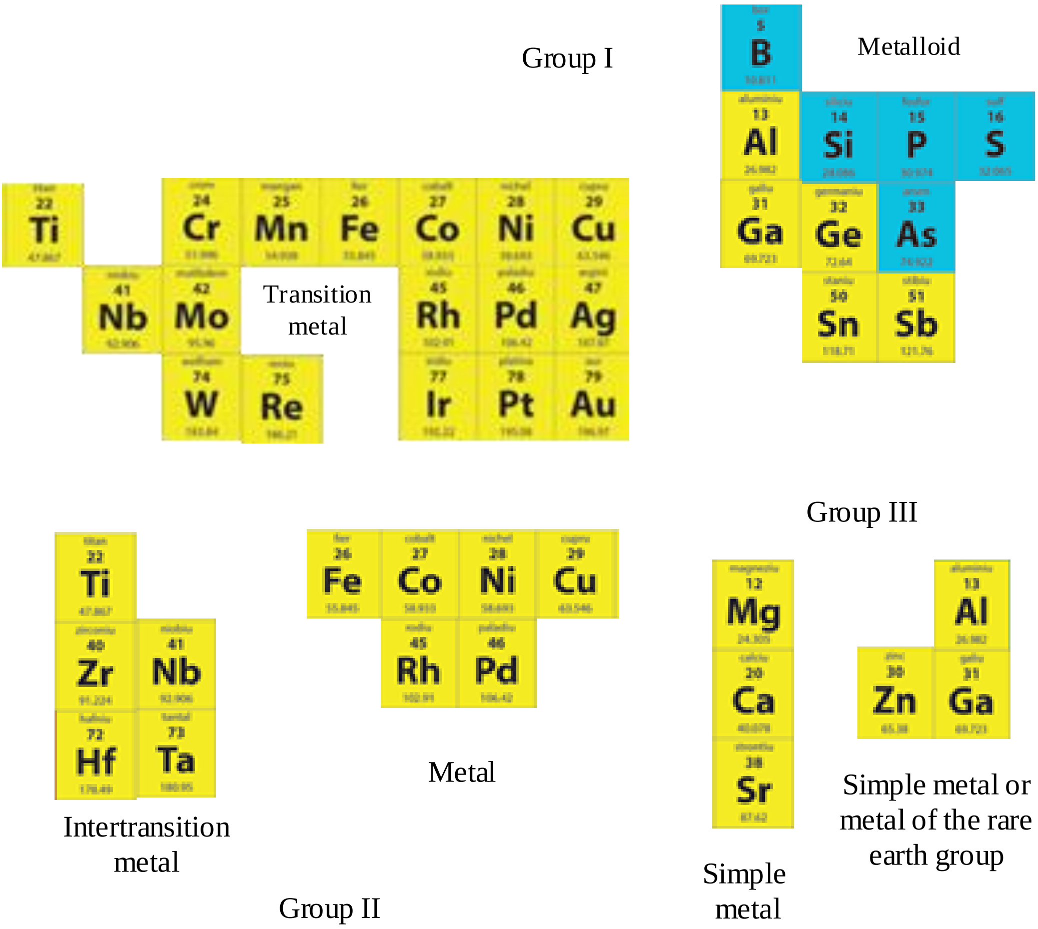

Figure 12. Groups of amorphous metals formed according to the positional criteria of the components: I - amorphous metal of the transition metal type (A) - metalloid (B); II - amorphous metal of intertransition metal type (A) - metal (B); III - amorphous metal of the simple metal type (A) - simple metal or metal of the rare earth group (B)

With the ultra-fast melt cooling technique, a wide range of amorphous metals can be obtained, to which different elements of the periodic table take part.
Alloys that have a high capacity to become amorphous are grouped into three groups, based on the position occupied by those components in the periodic table (Figure 12 [8]).

Table 1. Group I amorphous alloys

Nr. crt.	Components	Chemical composition / brand of amorphous metal
1.	Fe-Si-B	$Fe_{80}Si_5B_{15}$; $Fe_{77}Si_{10}B_{13}$; $Fe_{82}B_{12}Si_6$
2.	Fe-Si-B-C	$Fe_{81\ldots5}Si_{3\ldots5}B_{13}C_2$; $Fe_{80}Si_4B_{14}C_2$; $Fe_{67}B_{14}Si_8C_{11}$
3.	Fe-B Fe-B-Cr-Mo Fe-B-Cr-Bi-P	$Fe_{60}Cr_6Mo_6B_{28}$; Fe_aB_{100-a}(a =80-91%); $Fe_{42}B_6Bi_{26}Cr_{14}P_{12}$
4.	Fe-P-C Fe-P-C-B Fe-P-C-Cr	$Fe_{75}P_{15}C_{10}$; $Fe_aP_{10\ldots16}C_{5\ldots10}$; $Fe_{80}P_{10}C_3B_7$; $Fe_{72}Cr_8P_{13}C_7$;
5.	Fe-Ni-B-Bi Fe-Ni-B-Mo Fe-Ni-B-P	$Fe_{64}Ni_{14}Bi_8B14$ $Fe_{40}Ni_{38}Mo_4B_{18}$ $Fe_{40}Ni_{40}P_{14}B_6$
6.	Co-Fe-B Co-Fe-B-Si Co-Fe-B-Ni	$Co_{70}Fe_5Si_{15}B_{10}$ $Co_{74}Fe_6B_{20}$ $Co_{58}Ni_{10}Fe_5Si_{11}B_{16}$
7.	Ni-B Ni-B-Si	$Ni_{81}B_{19}$; $Ni_{75}Si_{18}B_7$;$Ni_{78}Si_{10}B_{12}$

The first group refers to amorphous metals formed by transition metals (A) and metalloids (B). It is recommended that the transition metals take part in atomic proportions of 75 ... 90%, and metalloids in atomic proportions of 25 ... 10%. The metalloids play the role of amorphous alloys. The most common alloys are ternary or multicomponent (Table 1 [8]).

The second group of amorphous metals consists of intertransitional components, i.e., transition metals of the first groups of the periodic table (A) and transition metals of the last groups of the table (B). (Ti, Zr, Hf, Nb, Ta) = (A) are used in various proportions together with the elements (Fe, Co, Ni, Cu, Rh, Pd) = (B). Table 2[8] lists some alloys in this group.

Table 2. Group II amorphous alloys

Nr. crt.	Components	Chemical composition / brand of amorphous metal
1.	Ti-Ni-Cu Ti-Ni-Co Ti-Ni-Fe Ti-Ni-Mn Ni-Zr	$Ti_{70}Ni_{20}Cu_{10}$ $Ti_{70}Ni_{20}Co_{10}$ $Ti_{70}Ni_{20}Fe_{10}$ $Ti_{70}Ni_{20}Mn_{10}$ $Ni_{90}Zr_{10}$
2.	Hf-Fe Hf-Co Hf-Ni	$Fe_{90}Hf_{10}$; $Co_{86}Hf_{14}$; $Ni_{88}Hf_{12}$
3.	Gd-Co Gd-Co-Mo	$Gd_{20}Co_{80}$; $Gd_{18}Mo_{10}Co_{82}$
4.	Cu-Zr(Ti) Cu-Ti	$Cu_{57}Zr_{43}$; $Cu_{50}Zr_{50}$; $Cu_{50}Ti_{50}$

The third group contains poly-component amorphous metals (Table 3 [8]) consisting of non-transition metals, accompanied or not by the rare earth metals (actinides and lanthanides).

Some components used to obtain amorphous alloys have an amorphous effect and are introduced into well-defined quantities. Thus, phosphorus has a favorable influence on the formation of amorphous alloys, but it increases their tendency towards fragility and reduces their polarization to saturation; the boron facilitates amorphousation and causes the stability of amorphous alloys over time; carbon is favorable for amorphousation and contributes to the thermal treatments and relaxation phenomena; silicon increases the stability of amorphous metals and improves magnetic properties.

Phase equilibrium diagrams provide information on compositional domains favorable to the formation of amorphous metal alloys. When analyzing the equilibrium diagrams of group I alloys, it is noted that the domain of favorable composition is around the eutectic concentration. At these alloys are present intermetallic compounds of the type A_3B, A_2B which are characterized by surrounding metalloid atoms by metal atoms, so that slightly distorted triangular prisms are formed. These structural units are maintained in amorphous metals as defining elements of local order at a short distance.

And in Group II alloys it is observed that the domain of amorphous composition is also around the eutectic concentration. In these alloys a strong amorphizing role is the existence of intermetallic phases such as Frank-Casper, Laves, etc., which have a very complex crystalline structure and are structural units to achieve the order at a short distance in amorphous state.

*Table 3.*Polycomponent alloys forming amorphous metals

Nr. crt.	Alloys
1.	Au-$Ge_{12\ldots17}$-$Si_{8\ldots12}$
2.	Pd-MN/$MT_{0\ldots66}$-$Si_{15\ldots22}$ MN/MT= noble metal, transition metal
3.	Fe-$MT_{0\ldots43}B_{16\ldots18}$ MT = one or more transition metals
4.	Fe-$Si_{8\ldots10}B_{12\ldots15}$ NiCo- $Si_{8\ldots10}B_{12\ldots15}$
5.	$Be_{30\ldots35}Ti_{6\ldots68}Zr_{0\ldots70}B_{0\ldots2}$ $Be_{30\ldots35}Ti_{6\ldots68}Zr_{0\ldots70}Al_{0\ldots2}$
6.	Fe-Ni-$MR_{0\ldots15}Si_{10}B_{12}$ $MR_{0\ldots15}Si_{10}B_{12}$ MR = one or more refractory metals
7.	Ta-$Ni_{25\ldots65}Ti_{0\ldots15}$;Ta-$Ni_{25\ldots65}Zr_{0\ldots15}$ Nb-$Ni_{25\ldots65}Ti_{0\ldots15}$; Nb-$Ni_{25\ldots65}Zr_{0\ldots15}$ W-$Ni_{25\ldots65}Ti_{0\ldots15}$; W-$Ni_{25\ldots65}Zr_{0\ldots15}$
8.	Mo-$Cr_{28\ldots45}P_{20}$; Mo-$Cr_{28\ldots45}$-B_{20} Mo-$Cr_{28\ldots45}$-C_{20}; Mo-$Cr_{28\ldots45}$-Si_{20} Mo-$Fe_{28\ldots45}$-P_{20}; Mo-$Fe_{28\ldots45}$-B_{20} Mo-$Fe_{28\ldots45}$-C_{20}; Mo-$Fe_{28\ldots45}$-Si_{20} Mo-$Ni_{28\ldots45}$-P_{20}; Mo-$Ni_{28\ldots45}$-B_{20} Mo-$Ni_{28\ldots45}$-C_{20}; Mo-$Ni_{28\ldots45}$-Si_{20} Mo-$Al_{28\ldots45}$-P_{20}; Mo-$Al_{28\ldots45}$-B_{20} Mo-$Al_{28\ldots45}$-C_{20}; Mo-$Al_{28\ldots45}$-Si_{20} Mo-$W_{28\ldots45}$-P_{20}; Mo-$W_{28\ldots45}$-B_{20} Mo-$W_{28\ldots45}$-C_{20}; Mo-$W_{28\ldots45}$-Si_{20}

9.	Fe-$B_{15...25}$; Fe-$Si_{15...25}$; Fe-$C_{15...25}$; Fe-$Al_{15...25}$ Ni-$B_{15...25}$; Ni-$Si_{15...25}$; Ni-$C_{15...25}$; Ni-$Al_{15...25}$ Co-$B_{15...25}$; Co-$Si_{15...25}$; Co-$C_{15...25}$; Co-$Al_{15...25}$ Cr-$B_{15...25}$; Cr-$Si_{15...25}$; Cr-$C_{15...25}$; Cr-$Al_{15...25}$
10.	U-$Cr_{0...40}$-$V_{20...40}$
11.	Nb-$Ir_{40...50}$; Nb-$Rh_{40...50}$; Ta-$Ir_{40...50}$; Ta-$Rh_{40...50}$
12.	$Ti_{45}Be_{40}Zn_{10}V$; $Ti_{45}Be_{40}Zn_{10}Cr$ $Ti_{45}Be_{40}Zn_{10}Mn$; $Ti_{45}Be_{40}Zn_{10}Fe$ $Ti_{45}Be_{40}Zn_{10}Co$
13.	Zr-$Co_{20...40}$; Zr-$Ni_{20...40}$; Zr-$Pd_{20...40}$

The formation of amorphous phases is favored when competing crystalline phases have complex structures with large numbers of coordinates and many different atomic locations [5]. Also, the existence of very stable intermetallic compounds in a certain compositional area of the phasic equilibrium diagram influences the formation of amorphous metal in the adjacent areas.

The group III alloys have both an amorphous-favorable composition domain around the eutectic concentration and the existence of intermetallic compounds.

According to the above, it results that in the binary alloys there appear both certain compositional domains favoring the formation of amorphous metals around the eutectic concentration and intermetallic phases.

To obtain amorphous structures, the poly-component alloys present experimentally established composition domains, positioned on isothermal sections of ternary or polyternary diagrams.

Below are analyzed the areas of composition which favors the obtaining of amorphous metals in the case of ternary and multi-component alloys.

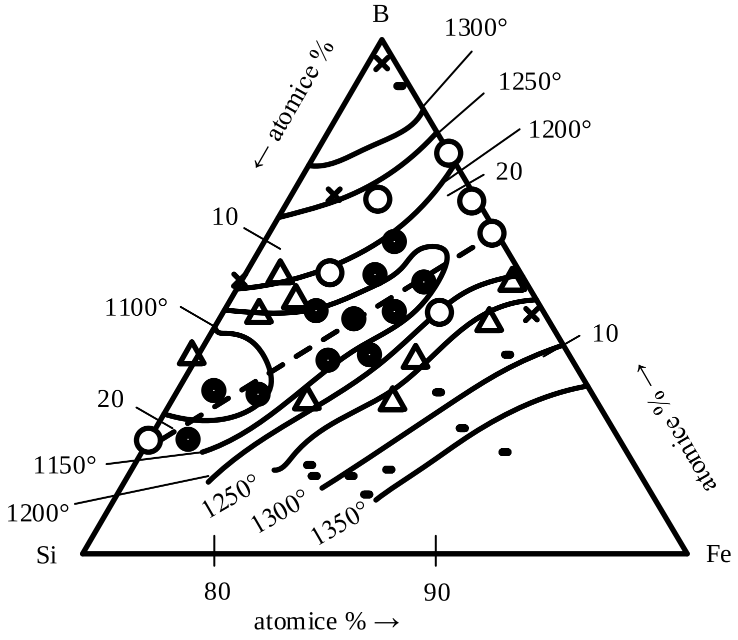

Fig. 13. Section in a Fe-Si-B ternary diagram

The composition domain that is favorable to the formation of amorphous metal for Fe-B-Si (Figure 13 [8]) is represented by the area of the black and white circles. Compositions in the black circle area give amorphous metals with a maximum thickness of 30 μm, and those corresponding to the white circle area give amorphous alloys with a thickness of 20 ... 30 μm.

Composition areas that are marked with points, triangles and crosses give alloys with a partial or total crystalline structure. Isotherms at various levels of liquidus temperature give additional information on the more favorable composition domain, i.e., areas of lower liquidus temperature.

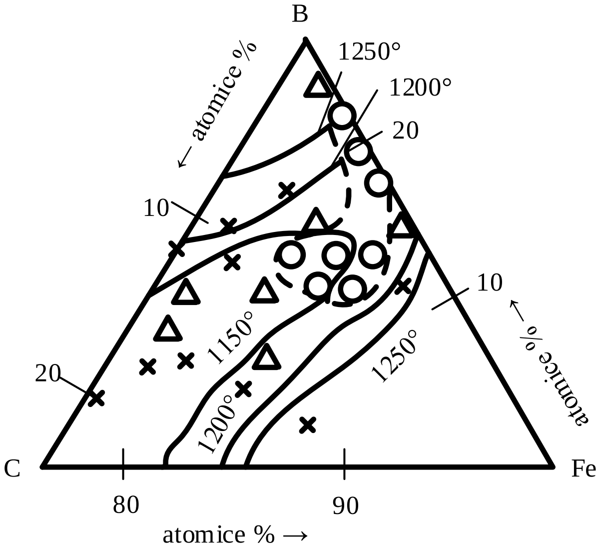

Fig. 14. Section in a Fe-B-C ternary diagram

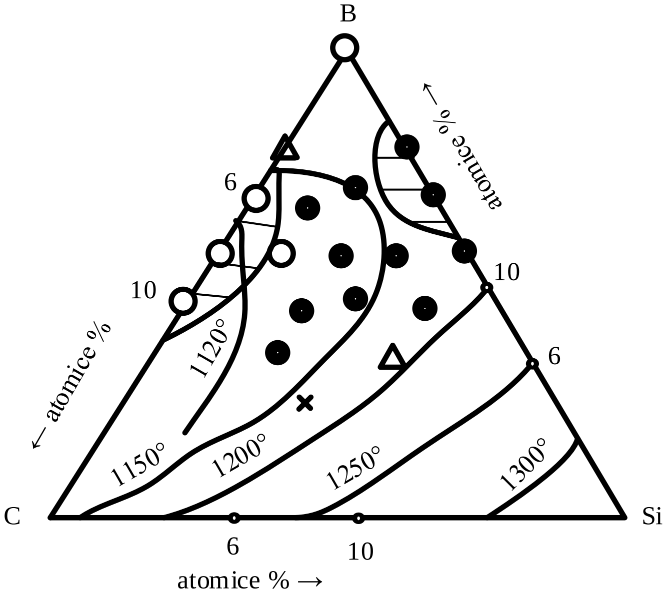

Fig. 15. Section in a Fe-Si-B-C diagram

In the case of the Fe-B-C alloy (Figure 14 [8]), the domain of composition that is favorable to amorphous formation is indicated by circles and the unfavorable one is signaled by triangles and crosses. In alloys with compositions close to the eutectic, if metalloids are added, the amorphizing capacity increases, because the metalloids raise the crystallisation temperature.

For the Fe-B-Si-C alloy (Figure 15 [8]), the composition which is favorable for amorphous alloying is shown by the area marked by the black circles; the hatched areas, also having low liquidus temperatures, become even more favorable for the amorphous state.

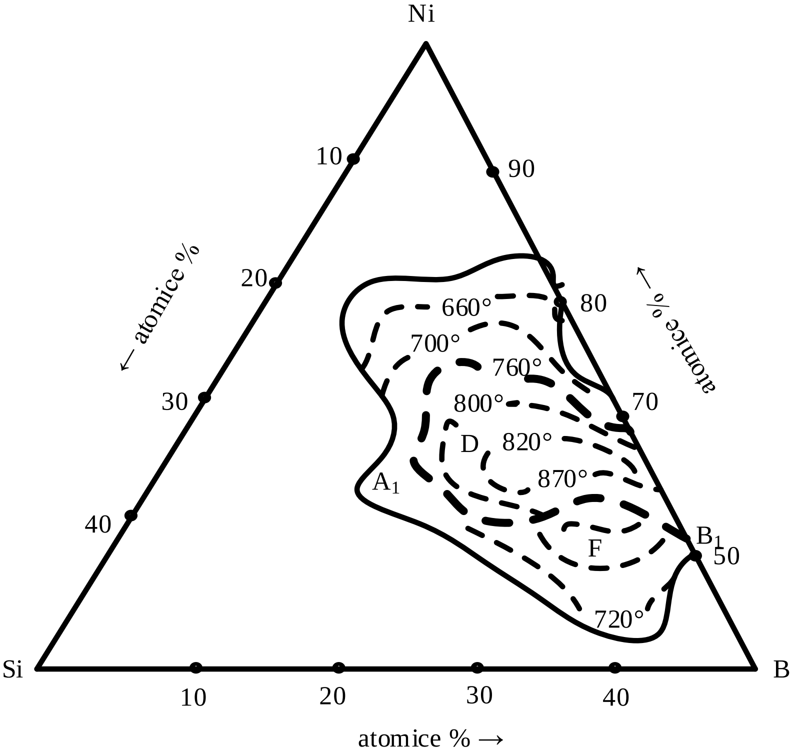

Fig. 16. Section in a Ni-B-Si ternary diagram

The Ni-B-Si alloys (Figure 16 [8]) have a favorable composition range in the isothermal imaging area. This area is divided into two areas of the A_1B_1 curve, which divide amorphous metals obtained in ductile (D) and fragile (F). The isothermal curves indicate the crystallization temperature (T_x) of the amorphous metal, expressed in [K]. In the field of composition represented, the amorphous metals obtained have a maximum thickness of 17 µm.

The amorphous metal forming capacity is also influenced by the crystallization temperature of the alloy. If the crystallization temperature (T_x) has high values, then an amorphous state may be obtained at higher fiber or strip thicknesses. For values of the ratio T_x/T_f = 0.52 ... 0.64 it's recording an increase in the alloying amorphizing capacity.

In conclusion, it is very important for the analysis of obtaining amorphous alloys to consider that their domain of compositions is around the eutectic concentration, to allow the formation of intermetallic compounds and to have the highest value of the T_x/T_f.

4. Conclusions

Due to the specific structure with short order of atoms, the amorphous metals present a homogeneity both on macro and microscopic scales. Strong interactions between the atoms of the components, exerted at a small distance, produce a range of unique and specific properties and behaviors. Thus, there is an association of mechanical properties of ductility and hardness, which do not occur in metallic crystalline materials. Amorphous metals have special magnetic, electrical properties and high corrosion resistance.

Due to this interesting set of properties, amorphous metals deserve attention for their industrial use, because they allow for the reduction of metal consumption with the crystalline structure.

CONSIDERATION ON AMORPHIC METALS

References

[1] Baum B. A. 1982 *Topituri metalice* Editura Tehnica Bucuresti

[2] Becherescu D. 1983 *Chimia starii solide* Editura Stiintifica si Enciclopedica Bucuresti

[3] Faigel G. 1980 *Quasi crystalina modeling of amorphous alloys* Conference on metallic glasses Budapesta

[4] Georgescu L. 1982 *Fizica starii lichide* Editura Didactica si Pedagogica Bucuresti

[5] Giessen B. G. 1972 *Liquid metals* Physics and Chemistry Dekker New York

[6] Radulescu M. 1982 *Studiul metalelor* Editura Didactica si Pedagogica Bucuresti

[7] Takacs L. Hargitai D. 1980 *Characterisation of the local order in amorphous* Conference on metallic glasses Budapesta

[8] Trusculescu M. s.a. 1988 *Metale amorfe* Editura Tehnica Bucuresti

[9] Vincze J. s.a. 1980 Physical Review nr B21 937

[10] Waterstriet R. M. s.a. 1979 *Nb-Si-Al_5 compounds produced by liquid quenching* Journal of Appl. Physic vol 50